Available online at www.sciencedirect.com

ScienceDirect

Procedia CIRP 00 (2016) 000–000

www.elsevier.com/locate/procedia

10th CIRP Conference on Intelligent Computation in Manufacturing Engineering - CIRP ICME '16

Densification mechanism for different types of stainless steel powders in Selective Laser Melting

Stefania Cacace[a]*, Ali Gökhan Demir[a], Quirico Semeraro[a]

[a]*Dipartimento di Ingegneria Meccanica, Politecnico di Milano, via La Masa 1, 20156, Milano (MI), Italy*

* Corresponding author. Tel.: +39-02-2399-8208; fax: +39-02-2399-8208. *E-mail address:* stefania.cacace@polimi.it

Abstract

Selective laser melting is a powder based additive manufacturing process where the metallic powder particles are melted by a high power laser beam. Different types of stainless steel powders made by gas and water atomization were analyzed before processing, in particular regarding their particle size distributions and morphology. Particle analysis was carried out using laser diffraction technologies and digital image analysis.
A suitable designed experiment has been carried out and the specimen density has been measured and linked to the properties of the powders. Eventually the possibility to reach high density specimen by adjusting process parameters is discussed.

Selection and peer-review under responsibility of the International Scientific Committee of "10th CIRP ICME Conference".

Keywords: Selective Laser Melting; Stainless steel powder; Densification

1. Introduction

Selective Laser Melting (SLM) is a laser based additive Manufacturing (AM) technology which allows to produce complex three-dimensional geometries directly from 3D CAD. The process starts from a fine metal powder which is spread upon a substrate metal plate, after a high-energy laser beam melts selectively the powder, in order to obtain one layer of the final object. The process repeats itself until the final part is completed.
SLM has received significant attention in the last years, due to its ability to overcome the limitations of traditional machining in terms of design freedom and manufacturing capabilities.
However, there are still some open questions about the improvement of surface quality, the dimensional accuracy and the achievable density. In this work the densification behaviour of different stainless steel powders is studied in the SLM process is studied. Powders are analysed according to their grain size distribution and shape. Specimen are produced with a self-produced SLM prototype and their density is evaluated.

2. State of the Art

The quality of an additive manufacturing produced part depends on many factors, the most important are build conditions and powder properties.
Build conditions are related to process parameters, object orientation in respect to the building platform, material etc. The influence of build conditions has been extensively studied in recent years [1-4]. On the other hand, the influence of powder properties on the final part has been recognized only in the recent past [5]. The uniformity of the powder layer affects the final part in terms of porosity and homogeneity of the bulk material. It is vital to understand which are the powder's characteristics related to its ability to be "spread" on the building plate [6].
The properties of metal powder depend on the atomization process, it is well-known that gas-atomized powders (GA) show quasi-spherical shape while water-atomized powders (WA) have irregular shape. This is the reason why gas atomized powders are preferred in the metal AM industry: spherical shape is supposed to guarantee high flowability properties. However flowability it is known to depend both on particle size distribution (PSD) both on shape. In particular, a

Selection and peer-review under responsibility of the International Scientific Committee of "10th CIRP ICME Conference".

high fine-fraction is not recommended because it generates agglomeration of particles and therefore a low powder bed density. As shown by Karapatis et al. [8] there are some considerations to be taken into account while studying the powder bed-density; in particular, it is demonstrated that a bi-modal distribution allows high packing-density since a high-fine fraction fills the void between larger particles. On the other hand, small particles (smaller than 15-10 µm) reduce the flowability of the powder. A compromise in the particle size distribution is needed in order to obtain high packing density and good flow properties. Starting from Karapatis results, Spierings et al [9] analysed the influence of different particle size distributions of stainless steel powders on the density of the final part. They showed that it is possible to produce fully-dense part with different grain size distribution when the process parameters are varied accordingly. They also analyse the relationship between particle size distribution and layer thickness. In their work some basic requirements to be fulfilled in order to obtain fully-dense part are given.

Gas atomized powder are generally preferred for additive manufacturing applications, nevertheless some work has been carried out to understand the differences between gas atomized and water atomized powders. Li et al [10] analysed stainless steel powders produced with different atomizing processes. Their work shows that higher laser power, lower scan speed, narrow hatch spacing and thinner layer thickness can improve density of the samples. The results of their analysis showed that parts produced with water atomized powder were characterized by high porosity. According to the authors this is due to the highest Oxygen content in WA powders and the lowest packing density in respect to gas atomized powders.

Similar results were obtained by Engel et al. [7], the authors studied the densification in the SLM process of strengthened superalloy In738LC. Eight different batches of powders were used during the experimentation, seven batches were gas atomized while one was water atomized.

They analysed powder in terms of: powder size distribution, mean diameter, shape and flow properties. The results show that flowability of the WA powders were lower, probably due to the irregular shape.

The parts produced with water atomized powder show high porosity (equal to 3%), while the average porosity of gas atomized samples was 1.2%.

The study of the relationship between Additive manufactured part properties (such as density, dimensional accuracy for example) depend on the type of powder and its characteristics. The possibility of producing fully dense part with different types of powders, in terms of granulometry and shape, by varying accordingly the process parameters is still an open question.

In this work the influence of two process parameters (Layer Thickness and Speed) and the production processes of the powder (Water and Gas atomization) on the density of test cube is investigated. The process parameters will be varied, and the density of the test samples will be evaluated with Archimedes method. Optical microscopy and X-ray computed tomography will be used in order to obtain further information about the densification behaviour in different conditions.

3. Materials and Methods

3.1. SLM Machine

The SLM machine used in this experimentation is a prototype developed at the Department of Mechanical Engineering at Politecnico di Milano. The machine consists of a laser source, a scanner, a sealed building chamber with a moving platform and a powder feeder.

The prototype is equipped with a multimode continuous wave IPG Photonics YLR-1000 laser with an El.En scan fiber head. In this configuration the beam diameter on focal plane is 212 µm. The maximum power of the laser source is 1000 W. The scanning velocity can be varied from 5 to 3000 mms^{-1} and the building area is 40x40 mm^2. In Table 1 the laser properties are listed.

A unidirectional scanning strategy was used to produce the specimens. For successive layers the direction of the scan line was not changed. Samples with 5x5x6 mm^3 dimension are build on a mild steel substrate. On each substrate 9 cubes were built with different process parameters, detailed in Section 3.4.

Table 1. Lase Properties

Parameter	Value
Wavelength	1070 nm
Maximum Power	1000 W
Fiber diameter	50 µm
Spot size	212 µm
Beam Quality factor (M^2)	5.4
Focal length	255 mm

3.2. Powders characterization

Water and gas atomized AISI 316L stainless steel powders were used in this work. For each type of powder, two different particle size distributions are available. Powder size distributions were analyzed using a Malvern Mastersizer 2000 laser diffraction machine. Figure 1 reports the measured particle distributions. The statistics for particle size distribution are in Table 2.

Powder shape was analyzed in a qualitative way with Zeiss EVO 50 Scanning Electron Microscope (Figure 2-3).

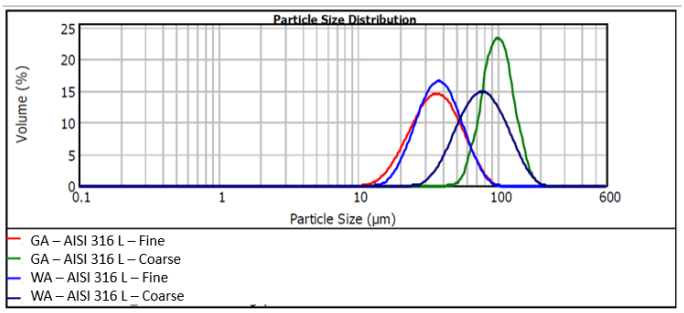

Figure 1. Particle Size distribution for 316L powders used in the experimentation.

In order to assess the variability in the distribution of the grain size, we define the span value as described by Engeli et al [7]:

$$Span = \frac{(D_{90} - D_{10})}{D_{50}}$$

Table 2. 316L powders used for the test specimens.

Type of powder	D_{10} [µm]	D_{50} [µm]	D_{90} [µm]	Span [-]
GA-AISI 316L-Fine	21.082	35.811	59.176	1.086
GA-AISI 316L-Coarse	72.138	99.291	137.510	0.638
WA-AISI 316L-Fine	23.747	37.504	58.875	0.936
WA-AISI316L-Coarse	46.201	76.489	125.669	1.039

Powders show a Gaussian-like distribution and the span value is equal to one except for GA-AISI316L-Coarse which shows a lower span.
As expected, different atomization processes induce different shape of the grains. GA powders show irregular and dendritic shape, while WA powders are mainly spherical with a small presence of satellites.

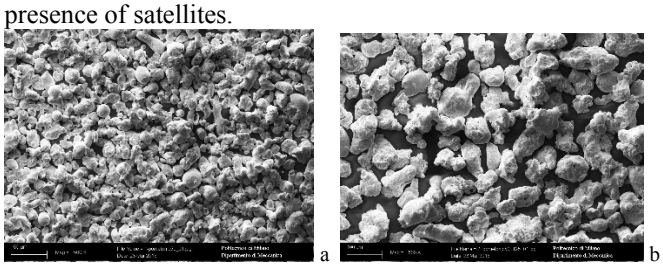

Figure 2. SEM pictures of WA powders. (a) WA-AISI 316L-Fine (b) WA-AISI 316L-Coarse

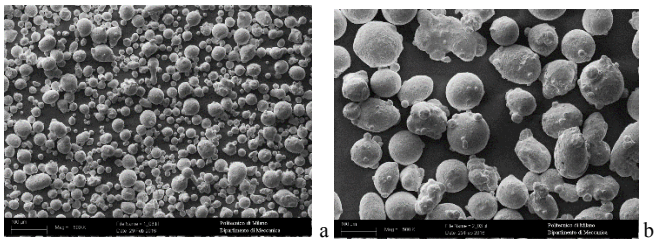

Figure 3. SEM pictures of GA powders. (a) GA-AISI316L-Fine (b) GA-AISI316L-Coarse

3.3. Test Cube characterization

All samples were characterized with optical microscope (Alicona Infinite Focus) in order to analyse the surfaces of the test cube and derive information about their density. Mean density was evaluated with Archimedes method. For the measurements an electronic balance with a Sartorius YDK 01 kit for the density measurement was used. The calculation of density (ρ) was performed according to the following formula:

$$\rho = \frac{W_a \cdot \rho_{fl}}{W_a - W_{fl}}$$

where W_a is the weight of the specimen in air, W_{fl} is the weight of the specimen in water and ρ_{fl} is the density of the water. The measurement were conducted in de-ionised water and the temperature dependence of ρ_{fl} with the temperature of the water was also taken into account. The measured density of each sample was compared to 7.98 g/cm^3, which is the expected density of AISI 316L according to [13].
Three test cubes were analyzed with computed tomography (North Star Imaging x25), the reconstruction software is efX-DR provided by NSI. In order to minimize beam hardening effects a 0.3 mm Cu filter was used during the acquisition. The zoom factor is x11.64 and the focal spot size is 5 µm. Scans of each sample were performed with 1440 projections over 360 degrees of rotation.

3.4. Experimental Design

The prototype allows the variation of several process parameters, such as laser power (P), scanning speed (v_s), distance between the consecutive scan lines namely hatch distance (h_d) and layer thickness (t). In this work the parameters which were varied are scan speed and layer thickness, according to Table 3.

Table 3. Process parameters of the current experimentation.

Process parameter	Levels
Scan speed, v_s [mm/s]	100-110-120-130-140-150-160-170-180
Layer thickness, t [µm]	50-100
Power, P [W]	263
Hatch Spacing, h_d [µm]	110

Hatch spacing and power were optimized for gas atomized AISI 316L powders in a previous experimentation. In that case the optimal speed was found to be 150 mm/s and 50 µm layer thickness.

The purpose of this work is to verify if the variation of process parameters (implicating a variation in the energy density) is sufficient to obtain dense part with powders with different particle size distribution and shape. Energy Density [J/mm^2] is defined as:

$$Energy\,density = \frac{P}{v_s \cdot h_d}$$

Energy density can be considered as the amount of surface energy given to the part during the process in the unit of time.

For each combination of powder type and layer thickness, a substrate with nine specimens was produced. A total number of 8 build jobs was performed for the experimentation. The nine cubes were scanned by forming a 3x3 grid on the substrate and the scan order has been studied in such a way that two neighboring cubes were not consecutively worked (Figure 4). This is to avoid the generation of temperature gradients in the substrate which could influence the deposition conditions. In respect to the test cube, Z denotes the building direction and X and Y denote the directions within the plate.

4. Density Analysis

In this section the result of the density measurement with the Archimedes method are shown.

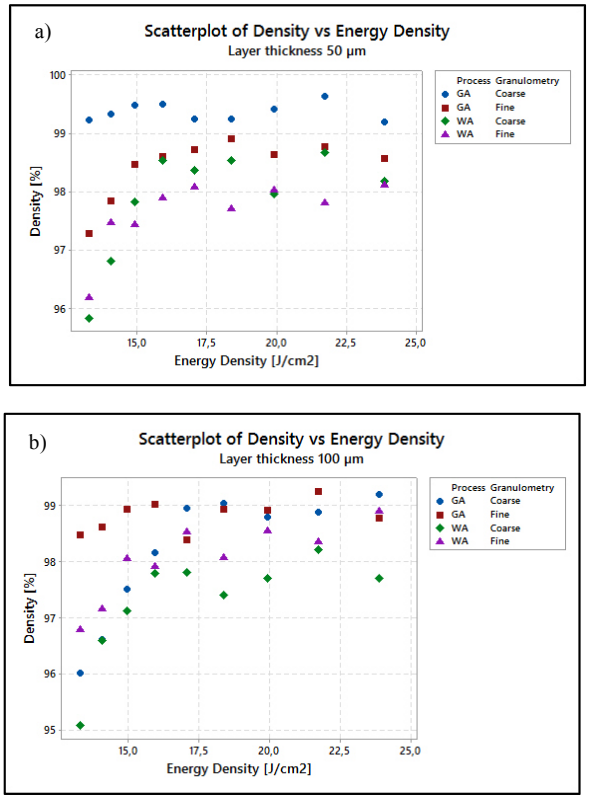

Figure 4. Plot of density [%] versus Energy Density [J/cm^2]. (a) Layer thickness equal to 50 µm, (b) layer thickness equal to 100 µm.

Table 4. Mean density obtained with different powders and layer thicknesses.

Type of powder	Mean Density t = 50 µm	Mean Density t = 100 µm
GA-AISI 316L-Fine	98.42 %	98.82%
GA-AISI 316L-Coarse	99.36 %	98.13%
WA-AISI 316L-Fine	97.63%	98.04%
WA-AISI316L-Coarse	97.86%	97.27%

The results show that with all the types of powder it was possible to produce test cubes with densities higher than 97% (Table 4). In Figure 4, densities of the nine test specimens are plotted versus the energy density. In Figure 4(a) and 4(b) the trend for all powders (except for GA-316L-Coarse at a layer thickness of 50 µm) shows an increase in density for low energy density, until a steady behavior is reached for higher energy input.

In figure 4(a), it can be clearly seen that at low energy density (corresponding to high speed), GA-316L-Fine, WA-316L-Fine and WA-316L-Coarse show low densities.

By decreasing the speed, the density of the samples becomes higher and reaches an asymptote, which is different for each powder. In particular, GA-316L-Fine performs better than water atomized powders.

On the other hand, GA-316L-Coarse shows a different behavior: the measured densities do not depend on the energy density, and even at high speed fully dense part were produced The same behavior is shown for samples produced at layer thickness equal to 100 µm, Figure 4(b). However in this case it seems that the steady behavior is reached at higher level of energy density in respect to the case of layer thickness equal to 50 µm. This is probably because a higher layer thickness needs higher energy in order to be fully melted.

In general, gas atomized powder perform better than water atomized ones. This result was expected, but it must be pointed out that even with water atomized powder it was possible to produce high-density part. In detail with the powder WA-AISI316L-Fine with a layer thickness equal to 100 µm, it was possible to obtain a density of 98.90% with a low speed (100 mm/s), and with the powder WA-AISI316L-Coarse with a low layer thickness, the maximum density was 98.67% at a scan speed of 130 mm/s. Probably, in order to overcome the disadvantage of WA powder (low flow properties and low packing density), the process should be slowed down, losing in productivity. Further experimentation with WA powder and lower scan speed is needed in order to verify this theory.

From Figure 4(a) and 4(b), it is possible to notice that at both levels of layer thickness, a minimum quantity of energy density should be delivered to the powder in order to obtain a high dense part. It appears to be a threshold level of energy density which should be exceeded in order to let the densification happen. In terms of productivity, it means that there is a lower level of speed we can use to perform the process and that depending on the layer thickness, the process should be slow down in order to be able to melt all the powder. A higher layer thickness also increases productivity, since fewer layers are needed to build part with the same height.

Another interesting feature is that fine fractions seem to perform better with the high level of layer thickness and, on the contrary, coarse fractions show better results with the low level of layer thickness. At low speed, it is possible that the energy received by smaller particles at 50 µm is enough for the evaporation process to take place, reducing the density of the final part. On the other side, bigger particles do not show good packing properties in correspondence with a high level of layer thickness because the voids between particles cannot be filled by the finer fraction. At low layer thickness, the biggest particle fill almost all of the space of the layer itself, leaving no room for voids. This could explain why coarser fractions shown better behavior at a layer thickness of 50 µm.

A statistical analysis is run in order to verify our considerations. The results of the ANOVA tests are shown in Table 5.

Since at high scan speed the process has not reached a steady behavior, the results for the scan speeds equal to 180 mm/s and 170 mm/s were removed from the analysis. Leaving out those two conditions gives us the opportunity to focus only on the steady behavior of the process. In this analysis, we looked at all the parameters of interest of our experiments: energy density layer thickness, granulometry and the production process of the powders. The analysis was performed with a significance level of 5%. Residuals of the model were checked: normality assumption cannot be rejected and all the standard residuals lie in the interval [-3;3].

The results confirm our conclusion about the significance of the production process on the density of the test samples. The interaction between layer thickness and granulometry is significant. This means that when dealing with different types of powder is important to change the process parameters in

order to obtain good results. The process parameters to be taken into account for the optimization of the density is not only speed but also layer thickness.
We can conclude that the better condition for high density are small layer thickness with a coarse granulometry and a high layer thickness with a fine powder fraction.

Table 5. ANOVA table for the density data.

Source	Adj SS	Adj MS	P-value
Production Process (GA-WA)	0.001019	0.001019	0.000
Layer Thickness	0.000036	0.000036	0.057
Granulometry (Coarse – Fine)	0.000005	0.000005	0.455
Energy Density	0.000162	0.000027	0.018
Layer thickness * Granulometry	0.000369	0.000369	0.000
Error	0.000422	0.000009	
Total	0.002012		

4.1. Internal Analysis

Test cubes were also internally characterized with X-ray tomography. All the slices shown in this section are taken in the X-Y plane. The scan properties are equal for all the samples. In particular, each reconstruction has a voxel size of 6.7 x 6.7 x 6.7 μm^3.

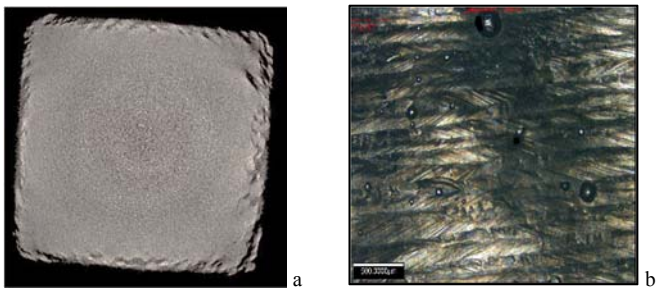

Figure 5. (a) Tomography of test cube produced with GA-AISI316L-Fine with layer thickness equal to 50 µm and speed 180 mm/s. (b) Optical microscopy of the surface of test cube GA-AISI316L-Fine with layer thickness equal to 50 µm and speed 180 mm/s.

In Figure 5(a) a slice of the sample GA-AISI316L-Fine. The test specimen shows a high-density and no-pore were detected during the scan. The optical image of the surface of this sample shows some balling, Figure 5(b), but no detection of balling can be seen from the slices. Balling is a surface phenomenon, but it can affect the homogeneity of the powder bed and therefore the porosity inside the sample.It is possible that balls formed during the process had no influence on the densification behavior, probably because they were re-melted during the scan of the next layer.

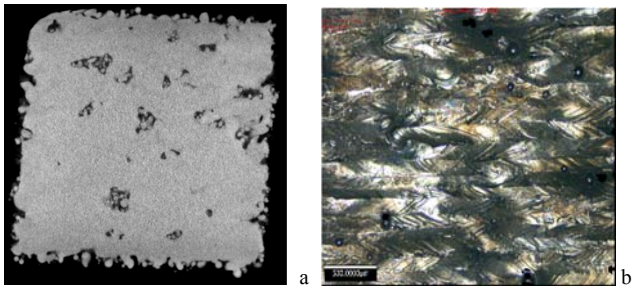

Figure 6. (a) Tomography of test cube GA-AISI316L-Coarse with a layer thickness equal to100 µm and speed 170 mm/s. (b) Optical microscopy of the surface of test cube GA-AISI316L-Coarse with a layer thickness equal to 100 µm and speed 170 mm/s.

In Figure 6 is reported a slice from the sample GA-AISI316L-Coarse with a layer thickness of 100 µm and a high speed. The sample shows a low density with big pores scattered within the sample. Looking at the slices it was evident that all the pores were connected along the Z direction for several consecutive layers.
By analyzing the slices from the X-ray tomography, spherical particles are evident inside the pores. Porosity could be due to sintered particles which were not melted during the process. Since the sample was produced at a high scan speed, the energy input might have been too low to melt the coarse powder in correspondence to a high layer thickness.
Porosity in the sample could be also due to the balling phenomena visible in Figure 6(b). The presence of metallic balls could prevent the homogeneous movement of the powder roller inducing the porosity on the layers.
The same pattern of porosity structure was detected also in samples produced with water Atomized powders. In Figure 7(a) a slice of the sample WA-AISI316L-Coarse with t=100 µm with high speed.

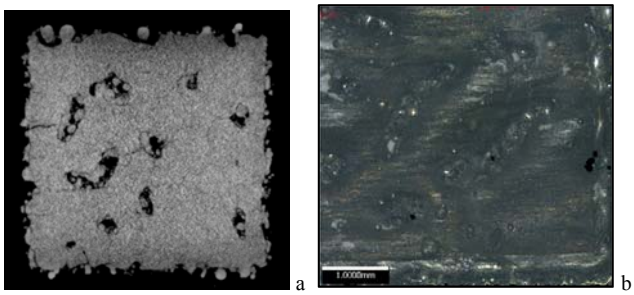

Figure 7. (a) Tomography of test cube produced with WA-AISI316L-Coarse with layer thickness equal to 100 µm and speed 170 mm/s. (b) Optical microscopy of the surface of test cube WA-AISI316L-Coarse with layer thickness equal to 100 µm and speed 170 mm/s.

In this case the surface shown in Figure 7(b) is more irregular: not only the scan lines are not visible, compared to the GA sample in Figure 6(b) but the upper surface is characterized by distinct peaks and valleys. The irregularity of the surface might imply that the lower flow properties of the WA powders affects the densification mechanism. In particular, the irregular shape of the particles might affect the deposition of the powder on the previous layer, preventing a homogeneous deposition by the rake.

5. Conclusions

In this work the influence of scan speed and layer thickness on the densification behavior of different powders types has been studied.
It was shown that, given the same processing conditions, gas atomized powders perform better compared to water atomized ones. The density increases as the Energy density increases until it reaches an asymptote.
Results show that the interaction between layer thickness and the particle size distribution is significant in order to describe the density of the part, as already shown by Spierings et al [9]. However, some critical points have to be taken into account: the presence of balling on the surfaces and the formation of big pores detected by XCT acquisitions.
Future work will be addressed to study the influence of other process parameters which identify the energy density (i.e. hatch spacing and power). A more detailed study on powders properties (i.e. flowability, tapped and apparent density) and their relationship with final part porosity and density is needed.

Acknowledgements

The authors would like to thank the AMALA laboratory for their support on the XCT analysis.

References

[1] Morgan, R., Sutcliffe, C. J., & O'neill, W. (2004). Density analysis of direct metal laser re-melted 316L stainless steel cubic primitives. Journal of Materials Science, 39(4), 1195-1205.
[2] Guan, K., Wang, Z., Gao, M., Li, X., & Zeng, X. (2013). Effects of processing parameters on tensile properties of selective laser melted 304 stainless steel.Materials & Design, 50, 581-586.
[3] Kruth, J. P., Froyen, L., Van Vaerenbergh, J., Mercelis, P., Rombouts, M., & Lauwers, B. (2004). Selective laser melting of iron-based powder. Journal of Materials Processing Technology, 149(1), 616-622.
[4] Simchi, A., & Pohl, H. (2003). Effects of laser sintering processing parameters on the microstructure and densification of iron powder. Materials Science and Engineering: A, 359(1), 119-128.
[5] Slotwinski, J. A., & Garboczi, E. J. (2015). Metrology needs for metal additive manufacturing powders. JOM, 67(3), 538-543.
[6] Dawes, J., Bowerman, R., & Trepleton, R. (2015). Introduction to the Additive Manufacturing Powder Metallurgy Supply Chain. Johnson Matthey Technology Review, 59(3), 243-256.
[7] Engeli, R., Etter, T., Hövel, S., & Wegener, K. (2016). Processability of different IN738LC powder batches by selective laser melting. Journal of Materials Processing Technology, 229, 484-491.
[8] Karapatis, N. P., Egger, G., Gygax, P. E., & Glardon, R. (1999, August). Optimization of powder layer density in selective laser sintering. In Proc. of Solid Freeform Fabrication Symposium 1999 (pp. 255-263).
[9] Spierings, A. B., Herres, N., & Levy, G. (2011). Influence of the particle size distribution on surface quality and mechanical properties in AM steel parts.Rapid Prototyping Journal, 17(3), 195-202.
[10] Li, R., Shi, Y., Wang, Z., Wang, L., Liu, J., & Jiang, W. (2010). Densification behavior of gas and water atomized 316L stainless steel powder during selective laser melting. Applied Surface Science, 256(13), 4350-4356.
[11] Mettam GR, Adams LB. How to prepare an electronic version of your article. In: Jones BS, Smith RZ, editors. Introduction to the electronic age. New York: E-Publishing Inc; 1999. p. 281-304.
[12] Li, R., Liu, J., Shi, Y., Wang, L., & Jiang, W. (2012). Balling behavior of stainless steel and nickel powder during selective laser melting process. The International Journal of Advanced Manufacturing Technology, 59(9-12), 1025-1035.
[13] UNI EN 10088 – 1:2014 . Stainless steels - Part 1: List of stainless steels